

INTRODUCTION AND MOTIVATION

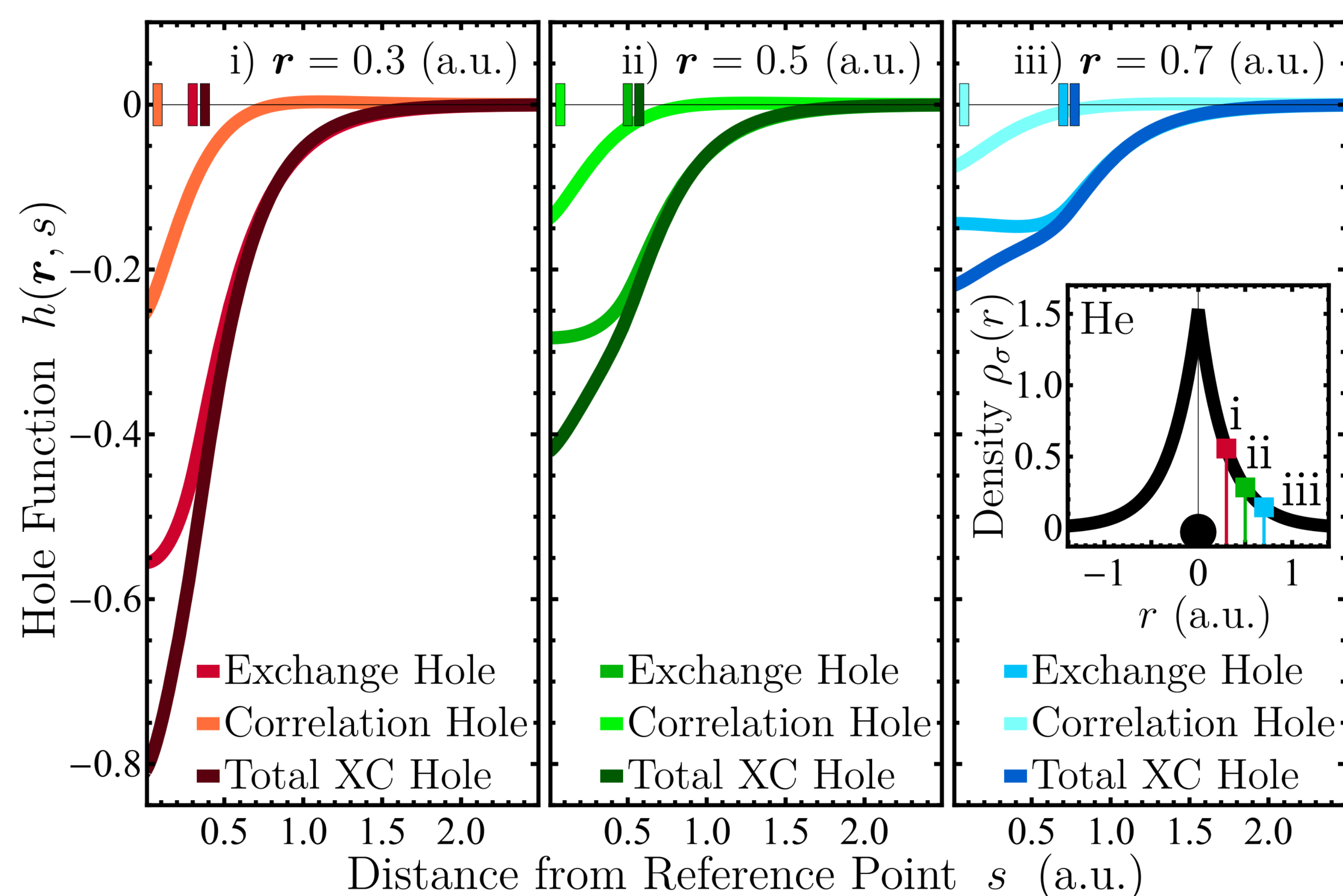
Density-functional theory (DFT) has become the workhorse of modern computational chemistry, with dispersion corrections (DCs) such as the exchange-hole dipole moment (XDM) model playing a key role in high-accuracy modelling of large-scale systems [1]. Here, we introduce physics-guided XDM variants: XCDM, which supplements XDM with same-

and opposite-spin dynamical correlation [2, 3], and XDM(Z), which implements the novel one-parameter damping function proposed by Becke to address shortcomings BJ-damping showed on alkali-metal clusters [4]. XCDM and Z-damping are now implemented in both Gaussian (via postg) and FHI-aims. XDM and its variants are benchmarked on the comprehensive GMTKN55

database [5] using GGA, global hybrid, and range-separated hybrid functionals, and compared directly to the D3(BJ), TS, MBD@rsSCS, and MBD-NL dispersion corrections. This marks the first time that the XDM and MBD corrections have been tested on GMTKN55. Four solid-state benchmarks testing molecular crystals are also considered.

CORRELATION CONTRIBUTION TO THE TOTAL XC HOLE

For the He atom, three different radial points are chosen for comparison as we plot the exchange hole, opposite-spin correlation hole, and the total exchange-correlation (XC) hole as a function of reference point s . Their associated dipole moment strengths are indicated with coloured bars along the s -axis. While the exchange hole is a reasonable approximation to the total XC hole, we see that the short-range dynamical correlation contribution is non-negligible and deepens it.



XCDM & Z-DAMPING IMPLEMENTATION

The XDM and XCDM models calculate the dispersion energy via a pairwise sum

$$E_{\text{disp}} = - \sum_{i < j} \sum_{n=6,8,10} \frac{f_n(R_{ij}) C_{n,ij}}{R_{ij}^n},$$

where f_n is a damping function, and $C_{n,ij}$ are heteroatomic dispersion coefficients are defined in terms of Hirshfeld-weighted atom-in-molecule polarizabilities and multipole moment integrals of the form

$$\langle M_\ell^2 \rangle_i = \sum_\sigma \int w_i(\mathbf{r}) \rho_\sigma(\mathbf{r}) [r_i^\ell - (r_i - d_{\text{XC}\sigma}(\mathbf{r}))^\ell]^2 d\mathbf{r}.$$

$d_{\text{XC}\sigma}(\mathbf{r})$ is the XC-hole dipole moment, obtained by supplementing d_X with same-spin ($\sigma\sigma$) and opposite-spin ($\sigma\sigma'$) correlation holes,

$$d_{\text{XC}\sigma} = \left(\int h_{\text{XC}\sigma} s ds \right) - \mathbf{r} = b_\sigma + \left[\frac{g_{\sigma\sigma} z_{\sigma\sigma}^7}{2 + z_{\sigma\sigma}} D_\sigma \right] + \left[\frac{g_{\sigma\sigma'} z_{\sigma\sigma'}^5}{1 + z_{\sigma\sigma'}} \rho_{\sigma'} \right] - \mathbf{r}.$$

The BJ-damping function, defined in terms of the “critical” interatomic distance at which successive dispersion energy terms become equal, and Z-damping, defined in terms of the atomic numbers, are given by

$$f_n^{\text{BJ}}(R_{ij}) = \frac{R_{ij}^n}{R_{ij}^n + (a_1 R_{c,ij} + a_2)^n}, \quad f_n^{\text{Z}}(R_{ij}) = \frac{R_{ij}^n}{R_{ij}^n + z_{\text{damp}} \frac{C_{n,ij}}{Z_i + Z_j}}.$$

The a_1 , a_2 , and z_{damp} parameters are optimised by minimising the RMS percent error in binding energies for a set of 49 molecular dimers.

WTMAD-4, GMTKN55, AND SOLID-STATE BENCHMARKS

Our analysis identified a flaw with the WTMAD-2, causing it to give subsets such as IL16 and DIPCS10 hundreds of times less weight than others, like BH76. We introduce WTMAD-4, which uses expected errors rather than energy scales for weighting, resulting in more balanced benchmark contributions.

$$\text{WTMAD-4} = \frac{1}{N_{\text{bench}}} \sum_{i=1}^{N_{\text{bench}}} w_i^{\text{WTMAD-4}} \cdot \text{MAD}_i$$

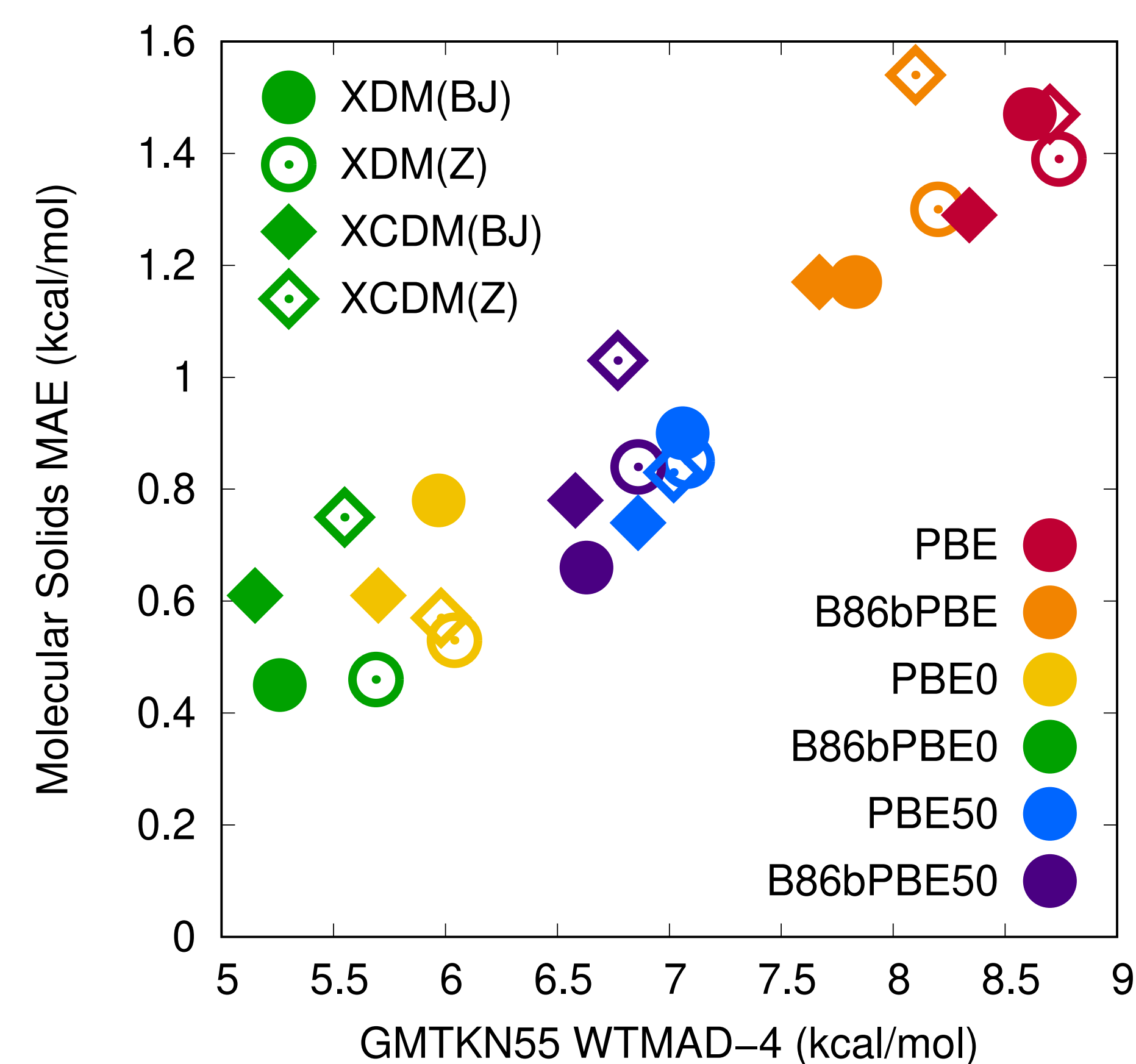
| | | |
|---------|-----|---|
| $w_i =$ | 50 | ACONE, RG18 |
| | 25 | ADIM6, Amino20x4, BUT14DIOL, HEAVY28, ICONF, MCONF, S66 |
| | 10 | BHROT27, HAL59, IL16, PCONF21, PNICO23, RSE43, S22, SCONF, UPU23 |
| | 5 | AHB21, CARBHB12, CDIE20, CHB6, ISO34, PAREL, TAUT15 |
| | 2.5 | AL2X6, BH76, BH76RC, BHPERI, BSR36, FH51, G21EA, HEAVYSB11, IDISP, INV24, ISOL24, NBPRC, PA26, YBDE18 |
| | 1 | ALK8, ALKBDE10, BHDIV10, DARC, DIPCS10, G21IP, G2RC, PX13, RC21, W4-11, WATER27, WCPT18 |
| | 0.5 | C60ISO, DC13, MB16-43, SIE4x4 |

GMTKN55 weighted MAD values (kcal/mol) for selected functionals and DCs:

| Functional | DC | WTMAD-2 | WTMAD-4 |
|------------------|----------|---------|---------|
| PBE0 | D3(BJ) | 6.60 | 5.87 |
| PBE0 | TS | 6.53 | 6.43 |
| PBE0 | MBDrsSCS | 6.45 | 6.12 |
| PBE0 | MBD-NL | 6.53 | 6.16 |
| PBE0 | XDM(BJ) | 6.55 | 6.06 |
| PBE0 | XDM(Z) | 6.96 | 6.12 |
| PBE0 | XCDM(BJ) | 6.23 | 5.79 |
| PBE0 | XCDM(Z) | 6.88 | 6.06 |
| B86bPBE0 | XDM(BJ) | 5.78 | 5.34 |
| B86bPBE0 | XDM(Z) | 6.43 | 5.73 |
| B86bPBE0 | XCDM(BJ) | 5.59 | 5.23 |
| B86bPBE0 | XCDM(Z) | 6.29 | 5.60 |
| LC- ω PBE | XDM(BJ) | 5.48 | 5.98 |
| LC- ω PBE | XDM(Z) | 5.51 | 5.92 |
| LC- ω PBE | XCDM(BJ) | 5.67 | 6.20 |
| LC- ω PBE | XCDM(Z) | 5.44 | 5.85 |

As shown, XCDM(BJ) is the most accurate dispersion correction paired with PBE0, and B86b exchange outperforms PBE, confirming the importance of the large-gradient limit. B86bPBE0-XCDM(BJ) and LC- ω PBE-XCDM(Z) appear best overall.

We also consider the X23, ICE13-Abs, ICE13-Rel, and HalCrys4 molecular crystal benchmarks. XCDM(BJ) achieved very low MAEs of 0.50–0.65 kcal/mol for all GGA and hybrid functionals tested using the `lightdenser` basis on X23, hinting at its use for CSP.



REFERENCES

- [1] A. D. Becke, E. R. Johnson, *J. Chem. Phys.* **127**, 15, 154108 (2007). doi: 10.1063/1.2795701
- [2] A. D. Becke, *J. Chem. Phys.* **88**, 2, 1053–1062 (1988). doi: 10.1063/1.454274
- [3] A. D. Becke, *Int. J. Quantum Chem.* **52**, S28, 625–632 (1994). doi: 10.1002/qua.560520855
- [4] A. D. Becke, *J. Chem. Phys.* **160**, 20, 204118 (2024). doi: 10.1063/5.0207682
- [5] L. Goerigk, A. Hansen, C. Bauer, S. Ehrlich, A. Najibi, S. Grimme *Phys. Chem. Chem. Phys.* **19**, 32184 (2017). doi: 10.1039/C7CP04913G

CONTACT INFO

KYLE BRYENTON
KBRYENTON@DAL.CA
PROF. ERIN JOHNSON
ERIN.JOHNSON@DAL.CA

